Probing the anomalous FCNC interactions in a top-Higgs boson final state and the charge ratio approach

Sara Khatibi and Mojtaba Mohammadi Najafabadi

School of Particles and Accelerators, Institute for Research in Fundamental Sciences (IPM), P.O. Box 19395-5531 Tehran, Iran

(Received 2 January 2014; revised manuscript received 7 February 2014; published 10 March 2014)

We study the anomalous production of a single top quark in association with a Higgs boson at the LHC originating from flavor-changing neutral current interactions in tqg and tqH vertices. We derive the discovery potentials and 68% C.L. upper limits considering leptonic decay of the top quark and the Higgs boson decay into a $b\bar{b}$ pair with 10 fb^{-1} integrated luminosity of data in proton-proton collisions at the center-of-mass energy of 14 TeV. We propose a charge ratio for the lepton in top quark decay in terms of lepton p_T and η as a strong tool to observe the signal. In particular, we show that the charge ratio increases significantly at large p_T of the charged lepton, while the main background from $t\bar{t}$ is nearly charge symmetric and the $W+$ jets background has much smaller charge ratio with respect to the signal. We show that this feature can also be used in the probe of anomalous single top production with a Z boson or a photon that is under the attention of the experimental collaborations.

DOI: 10.1103/PhysRevD.89.054011 PACS numbers: 12.39.Hg, 13.85.Rm, 14.80.Bn

I. INTRODUCTION

In view of the top quark large mass, it is a unique place to probe the dynamics that breaks the electroweak gauge symmetry. Several properties of the top quark have been measured and studied using the data collected with the LHC experiments at the center-of-mass energies of 7 and 8 TeV as well as the Tevatron experiments. The top quark interacts with other Standard Model (SM) particles via gauge and Yukawa interactions. So far, many remarkable results have come out of the LHC and Tevatron experiments including the top quark interactions in both electroweak and strong sectors. It is worth mentioning that both the ATLAS and the CMS experiments have measured several properties of the top quark with high precision [1,2]. In particular, the cross section for single top production has been measured with a precision of less than 15% [3], and the present measurement of the top pair rate is better than 10% [4]. Undoubtedly, it is expected that the top quark properties will be measured with more precision using more data and in the next phase of the LHC with collisions at 13 or 14 TeV.

Flavor-changing neutral current (FCNC) couplings are strongly suppressed in the top sector at tree level in the SM framework by the Glashow-Iliopoulos-Maiani mechanism [5], while the FCNC processes involving the top quark can appear in models beyond the SM. In particular, significant FCNC couplings of the top quark with an up or charm quark and a gluon are predicted in several new physics models beyond the SM [6–12]. The anomalous FCNC couplings for a top with an up-type quark (u, c) and a gluon can be described in a model-independent effective Lagrangian way according to the following [13,14]:

$$\mathcal{L} = \sqrt{2} g_s \sum_{q=u,c} \frac{\kappa_{tqg}}{\Lambda} \bar{t} \sigma^{\mu\nu} T_a (f_q^L P_L + f_q^R P_R) q G^a_{\mu\nu} + \text{H.c.} \quad (1)$$

Here P_L and P_R are chirality projection operators. In Eq. (1), Λ is the energy scale in which new physics appears and κ_{tqg} are real dimensionless parameters thus $\frac{\kappa_{tqg}}{\Lambda}$ are the strength of the couplings. The parameters f_q^L and f_q^R are chiral parameters with the normalization of $|f_q^L|^2 + |f_q^R|^2 = 1$. There are many analyzes in search for the anomalous tqg and other anomalous couplings related to the top interaction in the literature [15–20]. The CDF and D0 experiments at the Tevatron have searched for these FCNC couplings [21,22]. The 95% confidence level limits on the anomalous FCNC couplings have been found to be

$$\frac{\kappa_{tug}}{\Lambda} < 0.013, \qquad \frac{\kappa_{tcg}}{\Lambda} < 0.057 \text{ TeV}^{-1} \quad (2)$$

Recently, the ATLAS experiment set 95% C.L. upper limits on the strong FCNC couplings using 14.2 fb^{-1} of 8 TeV data. In the ATLAS search for the FCNC events in tqg vertex, the production of a single top quark with or without another light quark or gluon are considered [23]. The extracted limits are the most stringent limits on these couplings:

$$\frac{\kappa_{tug}}{\Lambda} < 5.1 \times 10^{-3}, \qquad \frac{\kappa_{tcg}}{\Lambda} < 1.1 \times 10^{-2} \text{ TeV}^{-1}. \quad (3)$$

The FCNC anomalous interaction tqg can lead to production of a top quark in association with a Z boson. In [24], a search for the top quark anomalous couplings has been performed through the search for the final state of a single top quark in association with a Z boson at the LHC with the

CMS detector. This search has been performed using 5 fb^{-1} of proton-proton collisions at 7 TeV data. The 95% C.L. observed upper limits on the anomalous couplings of the effective model are found to be

$$\frac{\kappa_{tug}}{\Lambda} < 0.1, \qquad \frac{\kappa_{tcg}}{\Lambda} < 0.35 \text{ TeV}^{-1}. \tag{4}$$

A lower cross section of this process and smaller amounts of data are the reason that these bounds are looser than the bounds with respect to the bounds indicated in Eqs. (2) and (3). However, performing such an analysis is necessary to check the consistency of all results in searches for FCNC. There is another detailed study for the anomalous interactions of tqg using; the tZ channel at the LHC with 20 fb^{-1} of 8 TeV collisions in [17]. The 3σ discovery ranges obtained in this study are as follows:

$$\frac{\kappa_{tug}}{\Lambda} > 0.09, \qquad \frac{\kappa_{tcg}}{\Lambda} > 0.31 \text{ TeV}^{-1}. \tag{5}$$

The discovery of a new Higgs-like particle with a mass of around 125 GeV by the ATLAS and CMS experiments at the LHC [25,26] has opened a new window in searches for different properties of SM particles. In particular, because of the large coupling of the Higgs boson with a top quark, the top quark properties could be studied in channels where a Higgs boson is also present. In this work, we perform a search for anomalous top interaction of tqg by studying a signature consisting of a Higgs boson and a single top quark. We perform the analysis for 10 and 100 fb^{-1} of the LHC proton-proton collisions at the center-of-mass energy of 14 TeV. We investigate the final state of three b jets where the top quark decays to a charged lepton (muon or electron), neutrino and a b quark and the Higgs boson decays into a $b\bar{b}$ pair. The representative Feynman diagram of the signal process including the decay chain is shown in Fig. 1 (left). In the final state we expect only one charged lepton, missing energy and three b-tagged jets. We find the parameter regions where the LHC may be able to observe the signal; otherwise, upper limits are set on the anomalous couplings. The real data of the LHC could be used in the search for the anomalous tqg couplings in this channel since it provides really reasonable results in comparison with the already obtained results from other channels even with a simple set of cuts. In order to improve the sensitivity to the tqg anomalous couplings, the tH channel results can be combined with both the FCNC single top quark and top pair production modes.

It is remarkable that for our favorite signal the radiation of a Higgs boson does not change the spin direction of the top quark. Therefore, if the anomalous interactions are quite left-handed ($f_q^L = 1$, $f_q^R = 0$) or right-handed ($f_q^L = 0$, $f_q^R = 1$), the top quark is produced with the spin direction parallel to the incident quark momentum direction for the left-handed case and opposite to the incident quark momentum for the right-handed case. The chirality information is transferred to the decay products of the top quark; accordingly, by a careful study of the charged lepton angular distribution, the type of interaction (left-handed or right-handed couplings) could be determined. Among the channels by which we can probe the anomalous tqg couplings, the direct top production [15] and top plus Higgs channel ($u(c) + g \to t + H$) provide the possibility to determine the chirality nature of these couplings. It is interesting to note that in addition to the effective FCNC Lagrangian in the vertex of tqg, introduced in Eq. (1), the anomalous FCNC interaction in the tqH vertex leads to production of a single top quark in association with a Higgs boson as well. This is illustrated by a Feynman diagram in the right side of Fig. 1, where flavor-changing interaction of the top quark and light quark involves a Higgs boson. The anomalous FCNC interaction tqH can be parametrized as the following [7]:

$$\mathcal{L} = \frac{g}{2\sqrt{2}} \sum_{q=u,c} g_{tqH} \bar{q} (g^v_{tqH} + g^a_{tqH}\gamma_5) tH + \text{H.c.}, \tag{6}$$

where the real coefficient g_{tqH} (with $q = u, c$) denotes the strength of the anomalous coupling. The coefficients g^v_{tqH}, g^a_{tqH} are, in general, complex numbers with the normalization $|g^v_{tqH}|^2 + |g^a_{tqH}|^2 = 1$. The 95% C.L. upper bounds on the FCNC tqH couplings derived from the low-energy experiments with the Higgs boson mass in the interval of 115 to 170 GeV are [27,28]

$$g_{tuH} < 0.363 - 0.393, \qquad g_{tcH} < 0.270 - 0.319. \tag{7}$$

In [16] the anomalous production of a single top quark with a Higgs boson via the FCNC, interaction of tqH has been studied at the LHC including complete QCD next-to-leading order corrections. The 3σ exclusion upper limits on the anomalous couplings with the Higgs boson mass of 125 GeV based on 10 fb^{-1} of the integrated luminosity have been found to be

$$g_{tuH} < 0.121, \qquad g_{tcH} < 0.233. \tag{8}$$

It is notable that both anomalous couplings tqg and tqH are arising from dimension-six operators. Therefore, it makes sense to consider both anomalous interactions together. The Feynman diagrams depicted in Fig. 1 can be studied simultaneously, which leads to an interference term. In this paper, we study the single top plus a Higgs boson final state once in the presence of only tqg couplings and once in the presence of both tqg and tqH anomalous interactions.

The organization of this paper is as follows. The next section is devoted to event simulation for signal (left diagram of Fig. 1) and backgrounds and analysis. In Sec. III we obtain the discovery potential and 68% C.L. upper limits on the anomalous couplings from this channel

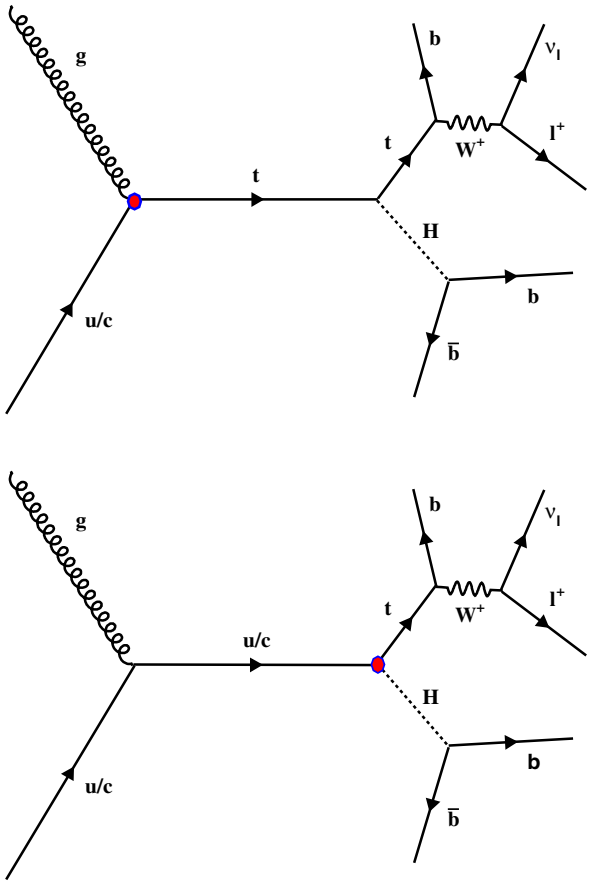

FIG. 1 (color online). The representative Feynman diagram for production of a top quark in association with a Higgs boson including the decay chain with leptonic top quark decay and Higgs decay into a $b\bar{b}$ pair.

and discuss the results. Section IV presents a simultaneous probe of tqg and tqH. In Sec. V, we will discuss a way, based on the leptonic charge ratio, to discriminate between signal and backgrounds and to distinguish between tug and tcg couplings. In particular, we look at the charge ratio as a function of p_T and η of the charged lepton for signal and background processes. Finally, conclusions are presented in Sec. VI.

II. EVENT SIMULATION AND SELECTION

In this section, we define the signal and backgrounds processes and describe the simulation method, the event selection, and reconstruction of the final state. The process of the signal is taken as the single top plus a Higgs boson followed by the leptonic top quark decay and the Higgs boson decay into a $b\bar{b}$ pair. The Feynman diagram of production and decay chain is presented in Fig. 1. The main background processes are $Wb\bar{b}j$, $Wjjj$, WZj, and $t\bar{t}$. For both the signal and background processes, the MADGRAPH 5 package [29] has been used to generate the hard scattering matrix elements with the CTEQ6 [30] as the parton distribution function. The parton level events are passed through PYTHIA 8 [31] for showering. The jet reconstruction is then performed by the FASTJET package [32] using an anti-k_t algorithm with the cone size of $R = 0.5$ [33]. Where $R = \sqrt{(\Delta\eta)^2 + (\Delta\phi)^2}$, with $\eta = -\ln\tan(\theta/2)$. The parameters η and ϕ are the polar and azimuthal angles with respect t the z axis. In this analysis, we focused on the LHC run with the center-of-mass energy of $\sqrt{s} = 14$ TeV for the integrated luminosities of 10 and 100 fb^{-1}. In order to simulate the signal events, the effective Lagrangian of Eq. (1) has been implemented with the FEYNRULES package [34,35], then the model was imported to a UFO module [36] and inserted in MADGRAPH 5. The cross sections have been found to be consistent with the COMPHEP package [37,38]. In this analysis, we only concentrate on the case that $f_q^L = f_q^R = 1$. The signal is generated with top quark decay leptonically (muon and electron) and the Higgs boson decaying into $b\bar{b}$. The $t\bar{t}$ background is generated in a semi-leptonic decay mode. The $Wb\bar{b}j$, $Wjjj$, WZj are generated with again leptonic decay of the W boson, and for the latter one the Z boson decays into a $b\bar{b}$. To simulate b tagging, a b-tagging efficiency of 60% is chosen for b jets and a mistagging rate of 10% for other quarks. The effects of detector resolution are simulated through Gaussian energy smearing, which is applied to jets and leptons with a standard deviation parametrized according to the following:

$$\frac{\sigma(E)}{E} = \frac{a}{\sqrt{E(\mathrm{GeV})}} \oplus b, \tag{9}$$

where $\sigma(E)$ indicates the energy resolution at the energy value of E, the symbol $\oplus$ represents a quadrature sum, and the energies are measured in GeV. For resolutions of jets (leptons), we take the values of the ATLAS detector [39], $a = 0.5(0.1)$ and $b = 0.03(0.007)$. It is notable that the electron and muon energy resolutions have different dependencies on the electromagnetic calorimetry and the charged particle tracking. Nevertheless, the uniform values for electromagnetic calorimetry energy resolution are used for the final state lepton. It is more conservative for the energies under consideration in the analysis than the capabilities of tracking. In order to trigger the events, every event is required to have at least one charged lepton passing through the cuts on the rapidity and transverse momentum. The typical value for the charged lepton p_T cut is 25 GeV within the pseudorapidity range of $|\eta| < 2.5$. The missing transverse energy is required to be larger than 25 GeV. The jets are required to have $p_T > 25$ GeV with pseudorapidities to be $|\eta| < 2.5$. The angular distance between the charged lepton and jets and all jets has to be $\Delta R_{lj,jj} > 0.4$. The cross sections of the signal after the above preliminary cuts including the branching ratios are

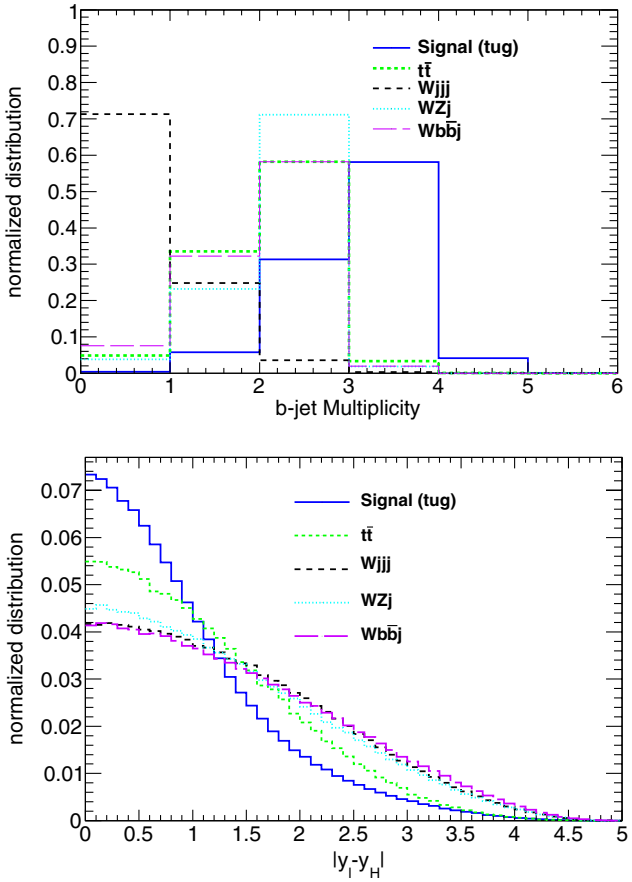

FIG. 2 (color online). The b-jet multiplicity distribution for signal and backgrounds (left) and the reconstructed distribution of $|y_l - y_H|$ for signal and different backgrounds. The distributions are normalized to one.

$$\sigma(\kappa_{tug}/\Lambda)\ \text{pb} = 5.60 \times \left[\frac{\kappa_{tug}}{\Lambda}\right]^2,$$
$$\sigma(\kappa_{tcg}/\Lambda)\ \text{pb} = 1.05 \times \left[\frac{\kappa_{tcg}}{\Lambda}\right]^2, \quad (10)$$

where κ_{tqg}/Λ is in TeV^{-1}. The process $Wjjj$ has the largest cross section, which is 230.0 pb, considering the cuts and branching ratios. The $t\bar{t}$ cross section after the cuts, and taking into account the branching ratios, is 34.35 pb. The cross sections of $Wb\bar{b}j$ and WZj processes are 2.33 and 0.138 pb, respectively. In order to reconstruct the top quark and Higgs boson in the final state, first we require that there be only three b-tagged jets in each event. The plot in the left side of Fig. 2 shows the b-jet multiplicity in signal and different backgrounds events. As can be seen, the requirement of only three b-tagged jets is useful to reduce the contribution of the backgrounds. We specifically apply such a requirement to suppress the large contributions of background events originating from $Wjjj$. To reconstruct the top quark, the full momentum of the neutrino is needed. The missing transverse energy is taken as the transverse component of the neutrino momentum. The z component of the neutrino momentum is obtained by using the W boson mass constraint: $(p_l + p_{T,\nu} + p_{z,\nu})^2 = m_W^2$. In most cases, there are two solutions for the $p_{z,\nu}$. As a result, the combination of the charged lepton and two neutrinos leads to two W bosons, which are combined with the three b-tagged jets separately. Among the six combinations, the combination which gives the closest mass to the top quark mass is selected. The other remaining two b jets are combined to reconstruct the Higgs boson.

In order to suppress the backgrounds, we reject events with $|m_{H,\text{rec}} - 125| > 15$ GeV. To reduce the contributions of the backgrounds and enhance the signal contribution, we exploit some other kinematic distributions. In the right panel of Fig. 2, the distribution of the difference between the pseudorapidities of the charged lepton and the reconstructed Higgs boson ($|y_l - y_H|$) is shown. The signal events prefer to reside mostly at around zero while the backgrounds, in particular the $W +$ jets events, have a more spread distribution and is extended up to around 5. Therefore, We require the events to satisfy $|y_l - y_H| < 1.2$ condition to reduce the $W +$ jets contributions. We use two

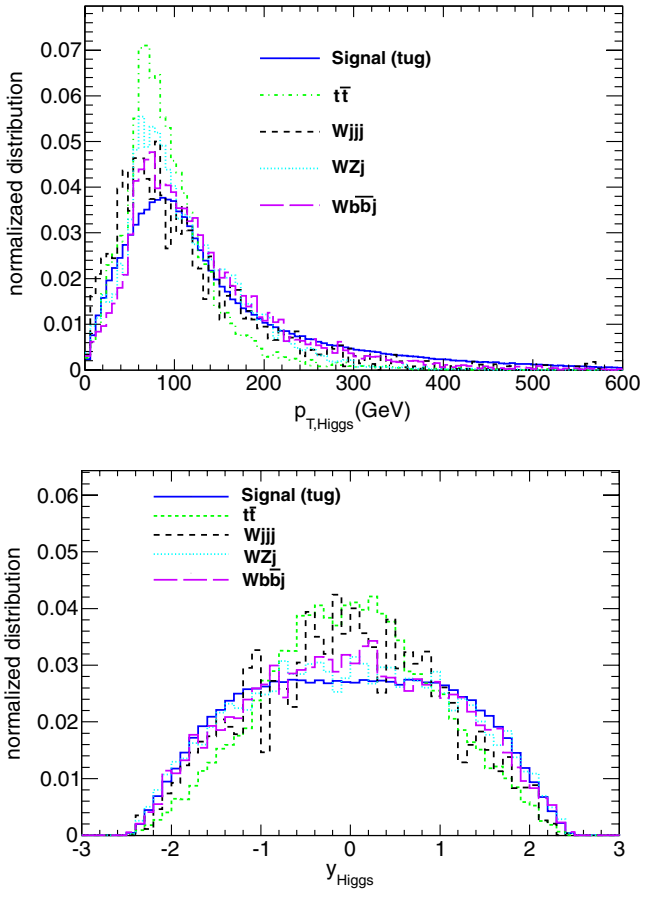

FIG. 3 (color online). The transverse momentum of the reconstructed Higgs boson (left) and the rapidity distribution of the Higgs boson (right) for signal and backgrounds.

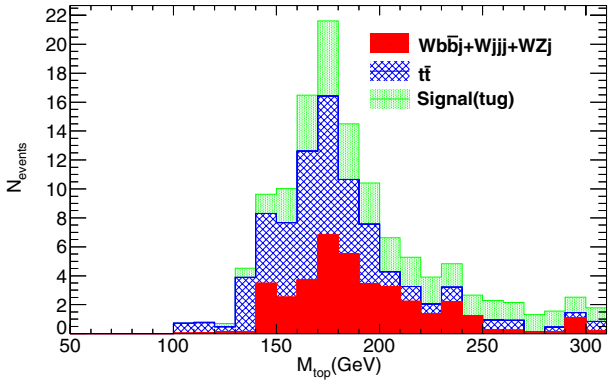

FIG. 4 (color online). The reconstructed top mass distribution after all selection for 10 fb^{-1} of LHC at 14 TeV center-of-mass energy for the signal with $\kappa_{tug}/\Lambda = 0.1$ TeV^{-1} and backgrounds.

more kinematic variables to suppress the backgrounds. In Fig. 3, the transverse momentum and rapidity distributions of the reconstructed Higgs boson are depicted. From the left panel of Fig. 3, we can see that in the $p_{T,\mathrm{Higgs}}$ distributions of $Wb\bar{b}j$, $Wjjj$, and WZj the peaks are below 80 GeV while for the signal the peak is around 90–100 GeV. Therefore, we require that the transverse momentum of the Higgs boson to be greater than 100 GeV. As it can be seen in the right panel of Fig. 3, for the signal process of $u + g \to t + H$, the Higgs bosons tend to reside also in the forward and backward regions while the main backgrounds of $t\bar{t}$ and $W +$ jets are mostly central. Since the up quark on average carries larger momentum with respect to gluon, the center-of-mass frame of the final state system is boosted along the direction of the initial up quark. We do not face with this situation for top pair events because the top pair events are mostly coming from gluon-gluon fusions which are symmetric. Only there is a small boost effect in top pair events due to quark anti-quark annihilation. We choose the events with $|y_H| > 0.8$. Because such an effect does not exist for the signal process of $c + g \to t + H$, we do not apply this cut for this process. In Fig. 4, we show the reconstructed top quark mass after all cuts for signal and backgrounds with 10 fb^{-1} of integrated luminosity and with $\kappa_{tug}/\Lambda = 0.1$ TeV^{-1}. It can be seen that top quark has been reconstructed well.

III. RESULTS

After applying all cuts that we explained in the previous section, we obtain the following efficiencies for signal ($\frac{\kappa_{tug}}{\Lambda} = 0.1$ TeV^{-1}), $t\bar{t}$, $Wb\bar{b}j$, $Wjjj$, and WZj, respectively: 12%, 0.017%, 0.04%, 0.0023%, 0.071%. For the tcg signal the efficiency has been found to be 6%. It should be mentioned that the $t\bar{t}$ process could also be considered as a source of top plus a Higgs boson. When one of the top quarks radiates a Higgs boson, the final state consists of $t\bar{t} + H$. Such events are unlikely to pass our selection. Because we require only one isolated lepton as well as exactly three b jets in the event which do not allow such events to contribute to the signal. We calculate the 3σ and 5σ discovery reaches of the LHC for the anomalous couplings $\frac{\kappa_{tug}}{\Lambda}$ and $\frac{\kappa_{tcg}}{\Lambda}$ after the event selection according to $S/\sqrt{B}$ formula. The 3σ (5σ) values for 10 fb^{-1} are summarized below:

$$\frac{\kappa_{tug}}{\Lambda} \geq 0.069\ (0.088), \qquad \frac{\kappa_{tcg}}{\Lambda} \geq 0.26\ (0.34)\ \mathrm{TeV}^{-1} \quad (11)$$

We see a better sensitivity to $\frac{\kappa_{tug}}{\Lambda}$ with respect to $\frac{\kappa_{tcg}}{\Lambda}$, which is because the parton density function of the charm quark is suppressed with respect to the up quark.

The next-to-leading order QCD corrections to signal would improve the results, however, the NLO corrections for our favorite signal are not available. If we assume a similar k factor of 1.3 as direct top production ($g + u(c) \to t$) [15] and $g + u(c) \to t + Z$ [40], the results mentioned above will improve up to the order of 10%. In case we find no evidence for the signal, upper limits can be set on the anomalous interaction parameters. To set the 68% C.L. limits, we use a simple χ^2 criterion from the distribution of $|y_l - y_H|$ with 10 fb^{-1} of the integrated luminosity. We perform the χ^2 on this distribution because the signal and backgrounds shapes are different and therefore could lead to stronger limits. The χ^2 criterion is defined as

$$\chi^2\left(\frac{\kappa_{u,c}}{\Lambda}\right) = \sum_{i=\mathrm{bins}} \frac{(s_i - b_i)^2}{\Delta_i^2}, \quad (12)$$

where s_i denotes the number of signal events in the ith bin of the $y_l - y_H$ distribution, and b_i is the number of background events predicted by the standard model in the ith bin. The χ^2 criterion depends on anomalous couplings of $\kappa_{u,c}/\Lambda$. In the χ^2 definition, $\Delta_i = b_i\sqrt{\delta_{\mathrm{stat}}^2 + \delta_{\mathrm{syst}}^2}$ where δ_{stat} is the statistical uncertainty and δ_{syst} denotes the term for considering systematic uncertainties. Systematic uncertainties from the top quark mass, PDF, factorization and renormalization scales, luminosity measurements, etc. are necessary for more realistic results. However, at this level of analysis it is difficult to give estimations of all systematics. Therefore, a combined systematic uncertainty of 10% is taken into account. The 68% C.L. upper limits on the anomalous FCNC couplings are found to be

$$\frac{\kappa_{tug}}{\Lambda} \leq 0.014, \qquad \frac{\kappa_{tcg}}{\Lambda} \leq 0.045\ \mathrm{TeV}^{-1}. \quad (13)$$

Certainly, these limits could be improved using advanced methods to separate signal from backgrounds such as neural networks [41] and boosted decision trees. The combination of the limits from this channel with other

channels also can lead to tighter bounds on the anomalous couplings.

In this analysis, we have not considered QCD multijet events. Because of its huge cross section, a data-driven technique is needed to estimate the contribution of this background. However, it is expected that the contribution of this background is negligible after the requirement of one isolated lepton and the missing transverse energy. Furthermore, requiring three b-tagged jets, where two of them must have a mass in the Higgs mass window, is expected to suppress the QCD background.

The SM single top plus Higgs, tZj, and $t\bar{t}Z$ events can also be sources of backgrounds to our signal. The inclusive LO cross sections are 52 fb, 0.55, and 1.02 pb, respectively. We have not included these backgrounds in the analysis due to very small cross sections. After including the branching ratios and applying the cuts, a negligible number of events will survive. One of the main backgrounds to this analysis is the $W+$ jets. The requirement of exactly three b jets suppresses this background dramatically. We expect that a full analysis with well-developed algorithms for b tagging provides more precise and reliable results. Therefore, a full detector analysis by the experimental collaborations is needed to confirm the results that we obtained in this analysis.

IV. SIMULTANEOUS PROBE OF tqg AND tqH COUPLINGS

The final state of the single top quark plus a Higgs boson can arise from both anomalous interactions tqg and tqH. Both anomalous couplings come from dimension-six operators. Therefore, in the presence of both couplings, the anomalous single top quark in association with a Higgs boson production cross section can be parametrized as

$$\sigma\left(\frac{\kappa_{tqg}}{\Lambda}, g_{tqH}\right)\ [\text{pb}] = c_{tqg} \times \left(\frac{\kappa_{tqg}}{\Lambda}\right)^2 + c_{tqH} \times g_{tqH}^2 + c_{\text{int}} \times \frac{\kappa_{tqg}}{\Lambda} \times g_{tqH}, \quad (14)$$

where κ_{tqg}/Λ is in TeV^{-1} and g_{tqH} is dimensionless. The coefficients c_{tqg}, c_{tqH}, and c_{int}. are determined with MadGraph. After the preliminary cuts described in Sec. II, the coefficients are $c_{tu(c)g} = 5.6(1.05)$, $c_{tu(c)H} = 0.09(0.01)$, and $c_{\text{int}} = 0.46(0.2)$. The numbers in parentheses denote the coefficients for the tcg and tcH couplings. As can be seen, the anomalous tqg coupling can have a larger contribution to the production of a single top quark in association with a Higgs boson. After applying similar requirements to what explained in the previous section the 3σ exclusion limits on the anomalous tqg and tqH are extracted. Figure 5 shows the 3σ exclusion regions in the plane of $(\kappa_{tqg}/\Lambda, g_{tqH})$ using 10 fb^{-1} of the integrated luminosity in proton-proton collisions at 14 TeV. In this plot, the smallest region shows the 3σ region for the anomalous interactions tug and tuH and the bigger one is the allowed region for tcg and tcH. Because of the smaller contribution to the signal cross section, looser bounds are obtained on the tqH couplings with respect to the tqg couplings.

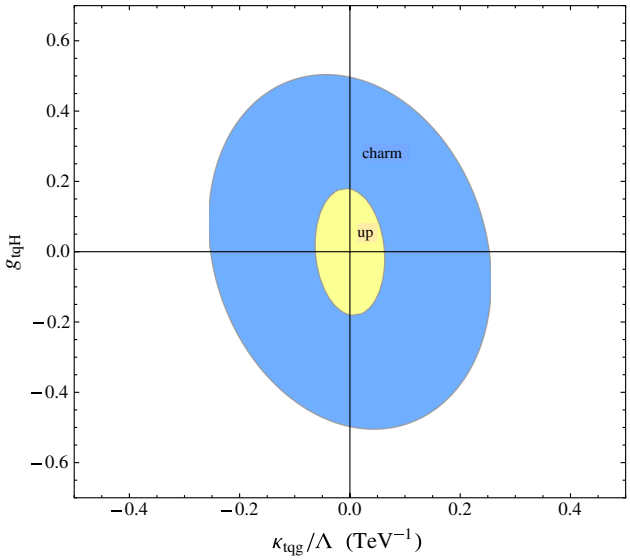

FIG. 5 (color online). The 3σ exclusion upper limits on the anomalous couplings $\frac{\kappa_{tqg}}{\Lambda}$ and g_{tqH} for 10 fb^{-1} of integrated luminosity at the LHC with the center-of-mass energy of 14 TeV.

V. CHARGE RATIO

One of the striking features of our signal, single top plus a Higgs boson production at the LHC, is asymmetry between top and antitop rates. The cross section of top and antitop quarks is different at the LHC for the process of $g + u(\bar{u}) \to t(\bar{t}) + H$ because of the difference between the u-quark and $\bar{u}$-quark parton distribution functions of the proton. Since the c-quark and $\bar{c}$-quark parton distribution functions are similar, the rates of top and antitop quarks from the process of $g + c(\bar{c}) \to t(\bar{t}) + H$ are expected to be similar. In leptonic top decay, the top/antitop asymmetry is directly translated in a corresponding lepton charge asymmetry. This is a reasonable assumption because the efficiencies of lepton selection and also fake charged lepton contamination are almost independent of charge. The dominant background to our signal is $t\bar{t}$, which is charge symmetric at leading order. However, when the next-to-leading order corrections are included, antitop quarks prefer to be more central than the top quarks. Therefore, more leptons will be observed than antileptons in the central region of the detector. The magnitude of this charge asymmetry is estimated to be around 1% [42]. The QCD multijet background is expected to be perfectly charge symmetric [43]. The only background that has charge asymmetry among the main backgrounds is $W+$ jets. This nice feature of the signal provides the possibility of

reaching the signal in the form of an excess in the ratio of positive to negative leptons after subtraction of the expected contribution of the $W+$jets background. In such an analysis one has to take into account the possibility of charge mis-measurement as well as any potential differences in efficiency between the positive and negative leptons. However, these are expected to be negligible, especially for muons. In this analysis, we define a ratio R as the number of events with positive charged lepton to the number of events with negative charge. The inclusive values of R for signal, $W+$jets ($W+jjj$ and $Wb\bar{b}j$), and $t\bar{t}$ are

$$\begin{aligned} R_{\text{signal}} &= 4.35 \pm 0.02, \\ R_{W+\text{jets}} &= 1.57 \pm 0.03, \\ R_{t\bar{t}} &= 1.04 \pm 0.03, \end{aligned} \tag{15}$$

where the uncertainties are only statistical uncertainties. As can be seen, the inclusive value of the charge ratio for the signal is significantly larger than the main backgrounds, even around three times larger than the ratio of the charge-asymmetric $W+$jets background. It is important to note that the value of R for the signal is independent of the value of the anomalous couplings κ_{tug}/Λ. A similar feature exists for direct top production due to anomalous tqg couplings, which has been discussed in [15]. In addition to the inclusive value of the charge ratio, we investigate the dependence of the charge ratio R for the signal and main backgrounds on the transverse momentum and pseudorapidity of the charged lepton. Figure 6 shows the charge ratio R as a function of lepton p_T (left) and lepton η (right). As can be seen, R grows with increasing the lepton p_T for the signal, while it is almost flat for $t\bar{t}$ and $W+$jets backgrounds. The charge ratio is around 3.8 for low p_T leptons, while it goes up to 5.4 for very energetic charged leptons. This behavior can be understood by considering the fact that the high p_T lepton in the final state needs a larger fraction of the parton momentum from the proton PDF. It is well known that the up-quark PDF are much larger than the anti-up-quark PDF at large values of x (x is the fraction of the proton momentum which a parton carries). Thus, at large lepton p_T, larger ratio is expected.

The ratio R as a function of lepton η is depicted in the right side of Fig. 6. Again for top pair events the ratio is almost flat and fluctuating around one, while for $W+$jets it is very slowly increasing with $|\eta|$. For the signal, R starts from 3.5 at $\eta \sim 0$ and grows significantly up to 6.8 at $2.0 \leq |\eta| \leq 2.5$. It is apparent that the ratio $R(p_T)$ and $R(\eta)$ has a strong discriminating power between the signal and the main backgrounds. The increasing behavior of the charge ratio with $|\eta|$ can be understood by looking at Fig. 7. As can be seen in this figure, there is an apparent correlation between p_T and η of the charged lepton for the signal events. Higher lepton p_T events are correlated with larger lepton η. Therefore, the large charge ratio for very energetic lepton would lead to the large charge ratio in the forward or backward region. Indeed, there is a correlation between $R(p_T)$ and $R(\eta)$.

It is important to note that the charge ratio is sensitive to the choice of parton distribution function (PDF) of the proton. In [43], the CMS Collaboration has measured the

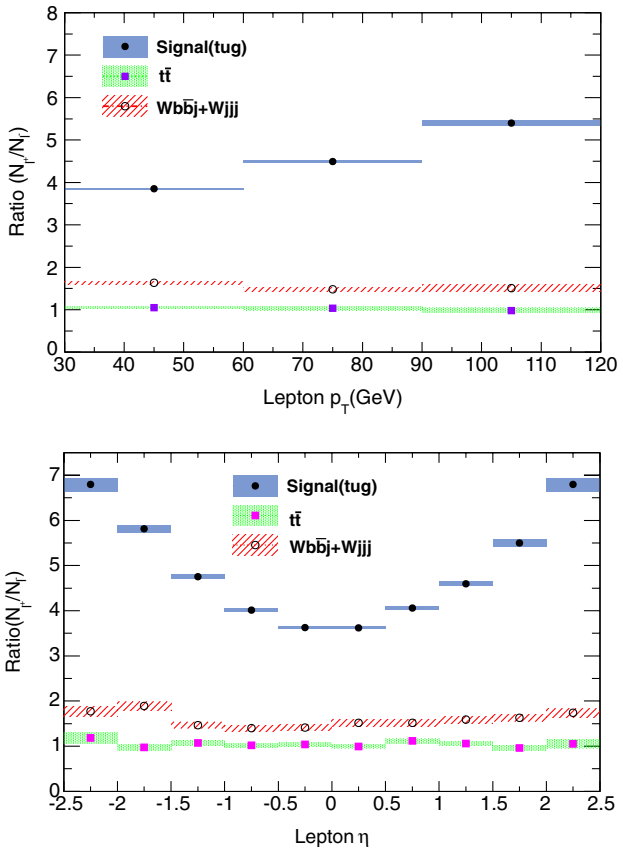

FIG. 6 (color online). The ratio of positive to negative leptons as a function of lepton p_T (left) and lepton η (right). The uncertainty is only a statistical one.

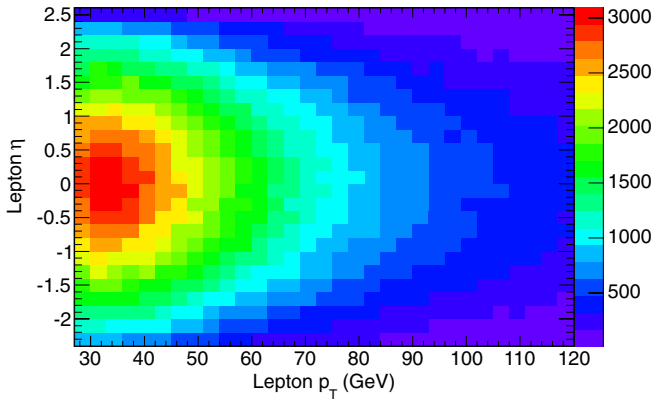

FIG. 7 (color online). The correlation between the transverse momentum and pseudorapidity of the charged lepton for signal events.

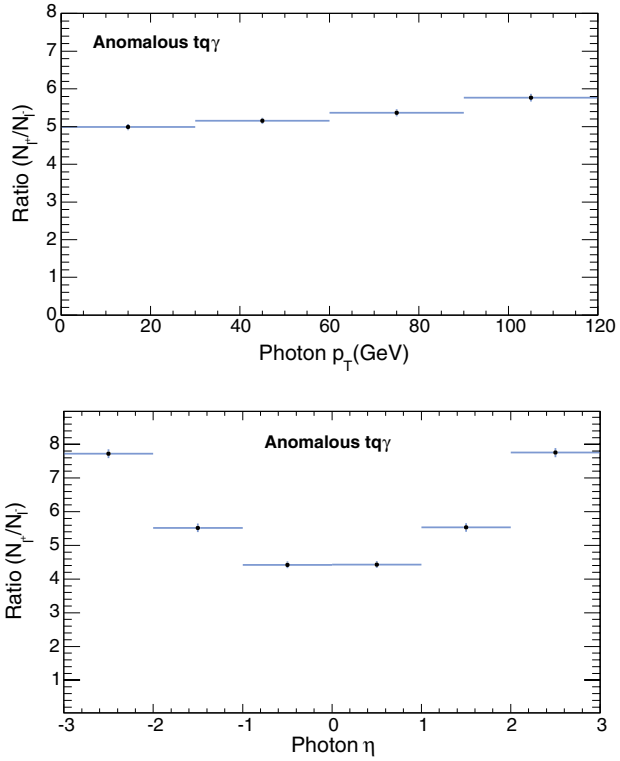

FIG. 8 (color online). The ratio of antilepton to lepton as a function of photon p_T (left) and photon η (right).

charge ratio in the single top t channel. The largest source of systematic uncertainty on the ratio is coming from the limited knowledge of the proton PDF. In this work, we have estimated the uncertainties due to the PDF by using the 44 members of the CTEQ6.6 PDFs. We have found that the relative uncertainty due to the PDF on the ratio R is around $\Delta R/R = 7\%$. The PDF uncertainty on the ratio R varies in bins of the lepton η. For the central leptons the PDF uncertainty is around 3% which increases up to around 6%–7% for the leptons in the forward or backward region. We also varied the factorization and renormalization scale to find uncertainty on the charge ratio. It is found to be less than 1%. Apart from the ability of the charge ratio to discriminate between signal and backgrounds, upon the signal discovery it can be used to determine that the signal comes from $t-u-g$ coupling or $t-c-g$ couplings. Since the $t-c-g$ anomalous coupling has equal contribution in top and antitop production, the inclusive and the differential charge ratio ($R(p_T)$ and $R(\eta)$) have quite different values and behaviors in the case where the signal originates from $t-u-g$ anomalous coupling. It is notable that similar charge ratio properties as mentioned in this section are applicable in the other channels of anomalous single top production in association with a vector boson or a Higgs boson—processes like $q+g\to t+\gamma$ (with anomalous interaction of $tq\gamma$ and tqg) and $q+g\to t+H$ (with anomalous couplings of tqH and tqg) and also $q+g\to t+Z$ (with anomalous interaction of tqZ and tqg) [16], [24], [17]. As an example, we show the charge ratio in the process of $q+g\to t+\gamma$ (with $tq\gamma$ anomalous interaction) as a function of photon p_T and η in Fig. 8. An increasing behavior for the charge ratio at large photon transverse momentum and large rapidities can be seen.

VI. CONCLUSIONS

In this paper we propose to use the $pp\to t(\bar{t})+H$ process to probe the anomalous tug and tcg couplings as a complementary channel in addition to the other channels. We concentrate on the leptonic decay of the top quark and the Higgs boson decay to $b\bar{b}$ at the LHC with the center-of-mass energy of 14 TeV. A set of kinematic variables has been proposed to discriminate between the signal from backgrounds. After applying the selection, we show that the LHC can probe the anomalous $tug(tcg)$ couplings down to $0.01(0.04)$ TeV^{-1} with 10 fb^{-1} of integrated luminosity. We also study the production of a signle top quark plus a Higgs boson coming from tqg and tqH anomalous couplings at the same time and derive the 3σ exclusion upper limits on the strengths of the anomalous couplings. We propose the charge ratio versus transverse momentum and the pseudorapidity of the charge lepton as a strong tool to discriminate between signal and backgrounds as well as its ability to distinguish between the anomalous couplings tug and tcg. We have shown that in particular in the high-p_T region or for the leptons in the forward or backward regions, the charge ratio increases significantly. We have found that the charge ratio is robust against the variation of the PDF and the Q scale.

[1] F.-P. Schilling, Int. J. Mod. Phys. A **27**, 1230016 (2012).
[2] W. Bernreuther, J. Phys. G **35**, 083001 (2008).
[3] The ATLAS Collaboration, ATLAS-CONF-2012-132.
[4] The ATLAS Collaboration, ATLAS-CONF-2012-024.
[5] S. L. Glashow, J. Iliopoulos, and L. Maiani, Phys. Rev. D **2**, 1285 (1970).
[6] T. M. P. Tait and C.-P. Yuan, Phys. Rev. D **63**, 014018 (2000).
[7] J. A. Aguilar-Saavedra, Acta Phys. Pol. B **35**, 2695 (2004).
[8] J. J. Liu, C. S. Li, L. L. Yang, and L. G. Jin, Phys. Lett. B **599**, 92 (2004).

[9] S. Bejar, J. Guasch, D. Lopez-Val, and J. Sola, Phys. Lett. B **668**, 364 (2008).
[10] J. Cao, Z. Heng, L. Wu, and J. M. Yang, Phys. Rev. D **79**, 054003 (2009); R. Guedes, R. Santos, and M. Won, *ibid.* **88**, 114011 (2013).
[11] G. A. Gonzalez-Sprinberg and R. Martinez, arXiv:hep-ph/0605335; R. Coimbra, A. Onofre, R. Santos, and M. Won, Eur. Phys. J. C **72**, 2222 (2012).
[12] J. A. Aguilar-Saavedra and B. M. Nobre, Phys. Lett. B **553**, 251 (2003); G. Eilam, J. L. Hewett, and A. Soni, Phys. Rev. D **44**, 1473 (1991); **59**,039901(E) (1998).
[13] E. Malkawi and T. M. P. Tait, Phys. Rev. D **54**, 5758 (1996).
[14] M. Hosch, K. Whisnant, and B. L. Young, Phys. Rev. D **56**, 5725 (1997); J. A. Aguilar-Saavedra, Nucl. Phys. **B812**, 181 (2009).
[15] J. Gao, C. S. Li, L. L. Yang, and H. Zhang, Phys. Rev. Lett. **107**, 092002 (2011).
[16] Y. Wang, F. P. Huang, C. S. Li, B. H. Li, D. Y. Shao, and J. Wang, Phys. Rev. D **86**, 094014 (2012).
[17] J.-L. Agram, J. Andrea, E. Conte, B. Fuks, D. Gel, and P. Lansonneur, Phys. Lett. B **725**, 123 (2013); J. A. Aguilar-Saavedra, Nucl. Phys. **B837**, 122 (2010).
[18] N. Kidonakis and A. Belyaev, J. High Energy Phys. 12 (2003) 004; P. M. Ferreira, O. Oliveira, and R. Santos, Phys. Rev. D **73**, 034011 (2006); J. A. Aguilar-Saavedra and G. C. Branco, Phys. Lett. B **495**, 347 (2000).
[19] S. M. Etesami and M. Mohammadi Najafabadi, Phys. Rev. D **81**, 117502 (2010); M. Khatiri Yanehsari, S. Jafari, and M. Mohammadi Najafabadi, Int. J. Theor. Phys. **52**, 4229 (2013).
[20] J. J. Zhang, C. S. Li, J. Gao, H. Zhang, Z. Li, C.-P. Yuan, and T.-C. Yuan, Phys. Rev. Lett. **102**, 072001 (2009).
[21] T. Aaltonen *et al.* (CDF Collaboration), Phys. Rev. Lett. **102**, 151801 (2009).
[22] V. M. Abazov *et al.* (D0 Collaboration), Phys. Lett. B **693**, 81 (2010).
[23] The ATLAS Collaboration, ATLAS-CONF-2013-063.
[24] The CMS Collaboration, CMS-PAS-TOP-12-021.
[25] G. Aad *et al.* (ATLAS Collaboration), Phys. Lett. B **716**, 1 (2012).
[26] S. Chatrchyan *et al.* (CMS Collaboration), Phys. Lett. B **716**, 30 (2012).
[27] A. Fernandez, C. Pagliarone, F. Ramirez-Zavaleta, and J. J. Toscano, J. Phys. G **37**, 085007 (2010).
[28] F. Larios, R. Martinez, and M. A. Perez, Phys. Rev. D **72**, 057504 (2005).
[29] J. Alwall, M. Herquet, F. Maltoni, O. Mattelaer, and T. Stelzer, J. High Energy Phys. 06 (2011) 128.
[30] J. Pumplin, D. R. Stump, J. Huston, H. L. Lai, P. M. Nadolsky, and W. K. Tung, J. High Energy Phys. 07 (2002) 012.
[31] T. Sjostrand, S. Mrenna, and P. Z. Skands, Comput. Phys. Commun. **178**, 852 (2008).
[32] M. Cacciari and G. P. Salam, Phys. Lett. B **641**, 57 (2006).
[33] M. Cacciari, G. P. Salam, and G. Soyez, J. High Energy Phys. 04 (2008) 063.
[34] N. D. Christensen and C. Duhr, Comput. Phys. Commun. **180**, 1614 (2009).
[35] C. Duhr and B. Fuks, Comput. Phys. Commun. **182**, 2404 (2011).
[36] C. Degrande, C. Duhr, B. Fuks, D. Grellscheid, O. Mattelaer, and T. Reiter, Comput. Phys. Commun. **183**, 1201 (2012).
[37] E. Boos, V. Bunichev, M. Dubinin, L. Dudko, V. Edneral, V. Ilyin, A. Kryukov, V. Savrin, A. Semenov, and A. Sherstnev (CompHEP Collaboration), Nucl. Instrum. Methods Phys. Res., Sect. A **534**, 250 (2004).
[38] A. Pukhov, E. Boos, M. Dubinin, V. Edneral, V. Ilyin, D. Kovalenko, A. Kryukov, and V. Savrin *et al.*, arXiv:hep-ph/9908288.
[39] G. Aad *et al.* (ATLAS Collaboration), arXiv:0901.0512.
[40] B. H. Li, Y. Zhang, C. S. Li, J. Gao, and H. X. Zhu, Phys. Rev. D **83**, 114049 (2011).
[41] M. Feindt and U. Kerzel, Nucl. Instrum. Methods Phys. Res., Sect. A **559**, 190 (2006).
[42] J. H. Kuhn and G. Rodrigo, J. High Energy Phys. 01 (2012) 063.
[43] The CMS Collaboration, CMS-PAS-TOP-12-038.